Organic & Biomolecular Chemistry

ROYAL SOCIETY OF CHEMISTRY

PAPER

View Article Online
View Journal | View Issue

Cite this: *Org. Biomol. Chem.*, 2023, **21**, 2941

Bioluminescence, photophysical, computational and molecular docking studies of fully conformationally restricted enamine infraluciferin†

Chia-Hao Chang,[a] Sandra Gómez,[b] Danielle M. Fontaine,[c] Panagiotis Fikas,[a] Bruce R. Branchini[c] and James C. Anderson *[a]

Received 15th February 2023,
Accepted 10th March 2023

DOI: 10.1039/d3ob00247k

rsc.li/obc

A new rationally designed fully rotationally restricted luciferin has been synthesised. This synthetic luciferin, based upon the structure of infraluciferin, has two intramolecular H-bonds to reduce degrees of freedom, an amine group to enhance ICT process, and an alkenyl group to increase π-conjugation. In the spectroscopic measurements and computational calculations, enamine luciferin showed more red-shifted absorption and fluorescence emission than LH_2 and iLH_2. With PpyWT luciferase enamine luciferin gave bioluminescence at 564 nm which is similar to LH_2 at 561 nm. Further investigation by docking studies revealed that the emission wavelength of enamine luciferin might be attributed to the unwanted twisted structure caused by Asp531 within the enzyme. With mutant luciferase FlucRed, the major emission peak was shifted to 606 nm, a distinct shoulder above 700 nm, and 21% of its spectrum located in the nIR range.

Introduction

Non-invasive bioluminescence imaging (BLI) with the luciferin-luciferase assay is one of the most popular methods for the non-invasive visualisation of biological process including detection, localisation and monitoring of *in vivo* and *in vitro* events.[1–3] Unlike fluorescence-based imaging, bioluminescence imaging provides visible photons without an external excitation source which negates noise and interference from unnecessary light scattering. As a result, bioluminescent probes have very low background signals, in comparison to fluorescence probes, resulting in high signal to noise ratios. Based on this unique property, bioluminescent probes can be used for highly sensitive and accurate bioimaging.[4] The most well-studied bioluminescence system consists of firefly luciferin, also called D-luciferin (**1**, LH_2), and firefly luciferase (Fluc) pairs. In the presence of oxygen, Mg^{2+} ions and adenosine triphosphate (ATP), D-luciferin is catalytically oxidised by its luciferase to generate an oxidised form oxyluciferin **2** in its excited state. The excited state ketone species relaxes to its ground state and emits a quantised photon of light (Scheme 1).[5] The emission wavelength ranges from 530 nm to ~630 nm depending on subtle differences in luciferase mutants and pH.[6] The bioluminescence quantum yield ($Ø_{blu}$) of D-luciferin is very high, determined to be 0.41 by total-photon-flux measurement.[7] However, the wavelength of light emitted by D-luciferin is readily absorbed by melanin, haemoglobin and tissue, which compromises the resolution of BLI in mammals. To improve tissue penetration and obtain better resolution, red-shifted emissions, especially in the near Infrared (nIR) range (λ_{blu} = 650 nm to 800 nm), is desirable. There have been many efforts towards this goal, historically by the development of mutant luciferases and more recently by the synthesis of D-luciferin analogues. A number of mutant luciferases have been reported[8–11] that allow D-luciferin to express different wavelengths of emitted light and shifting the emission wavelength above 600 nm. However, there is a limitation to this approach due to the inherent structure of D-luciferin allowing red shifting only so far. The synthesis of D-luciferin analogues has given bioluminescent molecules with far greater red shifted emission (*vide infra*), but due to their often-compromised stability, the development of rapid and efficient synthetic methods is slow and challenging. In addition, the

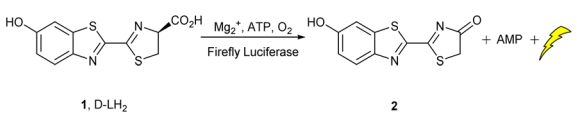

1, D-LH_2 2

Scheme 1 Adenylation and oxidation of D-luciferin to give firefly bioluminescence.

[a]*Department of Chemistry, University College London, 20 Gordon Street, London, WC1H 0AJ, UK. E-mail: j.c.anderson@ucl.ac.uk*
[b]*Departamento de Quimica Fisica, University of Salamanca, 37008, Spain*
[c]*Department of Chemistry, Connecticut College, New London, CT 06320, USA*

†Electronic supplementary information (ESI) available: General experimental, optimising reaction conditions for **13**, docking studies method and copies of ^1H and ^{13}C NMR, and IR spectra of new compounds. See DOI: https://doi.org/10.1039/d3ob00247k

random modification of the D-luciferin skeleton can result in the loss of bioluminescence activity with different luciferase variants.[12–15] Therefore, the synthesis of novel D-luciferin analogues which are compatible with luciferases is important for the development of new red shifted bioluminescent probes for application in deep tissue imaging.

Over the past few decades many synthetic luciferin analogues that exhibit red shifted light emission have been designed and synthesised (Fig. 1). White, who was a pioneer in bioluminescence research, demonstrated that the 6-hydroxyl group of D-luciferin could be replaced by a primary amine. The introduction of the more electron donating amino group in place of the naturally occurring hydroxyl group resulted in amino luciferin **3** giving red-shifted light emission (λ_{blu} = 593 nm), in part due to increasing intramolecular charge transfer. Unfortunately, **3** gave a much reduced light output compared to D-luciferin of about 10%.[16] Developing this concept further, Miller[17,18] synthesised a series of more electron donating alkyl and cyclic amino substituted luciferins which exhibited emission wavelengths above 600 nm. Among these analogues, a pair of Cycluc10 **4** and mutant luciferase R218K had the longest wavelength at 648 nm which was close to nIR. Although matching the analogue with a luciferase mutant to give the longest wavelength of emission, this cyclic analogue was 2–3 orders of magnitude less bright than D-luciferin. In 2012, Conley reported amino selenium luciferin **5** which gave bioluminescence emission at 600 nm, but its quantum yield was about 74% compared to amino **3** due to the heavy atom effect.[19] In 2013, Maki and co-workers developed non-benzothiazole extended luciferin **6** bearing two double bonds between the aromatic ring and the thiazoline.[20] With wild type luciferase, luciferin **6** showed nIR emission at 675 nm. Inspired by Maki's work, in 2014 we reported the synthesis of *infra* luciferin (**7**, iLH_2), a π-extended version of D-luciferin, which has a bridging alkenyl group between the benzothiazole and thiazoline ring systems of D-luciferin.[21] This π-extended luciferin provided nIR emission up to 730 nm with mutant CBR2.[11] As the structure retained the 6-hydroxyl group, it was also shown to be sensitive to colour modulation. Later this was capitalised upon by demonstrating nIR dual bioluminescence imaging in mouse models of cancer. However, like other D-luciferin analogues, iLH_2 suffered from reduced light output (~1000 times less bright than D-LH_2) and lower bioactivity with respect to D-luciferin.[22] In 2018, Hall reported the installation of an extra aromatic ring fused to the benzothiazole moiety to increase the π-conjugation of the natural system. With mutant luciferase CBR2, NH_2-$NpLH_2$ **8** showed nIR emission at 730 nm which was shown to be useful for deep tissue bioluminescence imaging and tomography. *In vivo* studies of NH_2-$NpLH_2$ **8** demonstrated greater cell membrane permeability in mice brain cells.[23] However, the intensity of light output was again weak (~5000–500 000 fold less than D-luciferin). In an attempt to increase light output by reducing radiationless decay from freely rotating bonds, we have synthesised rigid benzimidazole *infra*-luciferin analogue **9** that has reduced degrees of freedom around one of the linking alkene groups single bonds due to a covalent linker. With mutant luciferase x11, luciferin **9** had nIR bioluminescence at 714 nm with 5 times higher photon flux than its rotationally un-restricted form **10** at 561 nm. These results indicated that rigidification benefited longer emission wavelength and stronger light output. However, luciferin **9** was still 10 times less bright than iLH_2, and ~1000 weaker than D-LH_2 with mutant ×11.[24] More recently, Yao and co-workers described a partially restricted luciferin (**11**, PHOH-Luc) in which one of the linking groups single bonds was rotationally restricted by an intramolecular H-bond.[25] According to the fluorescence study, luciferin **11** gave a longer fluorescence wavelength at 569 nm than its rotationally un-restricted form Ph-Luc **12** at 445 nm suggesting that the interlocking H-bond provided a more planar π-conjugated system in its excited state. Additionally, density functional theory (DFT) calculation of luciferin **9** indicated that nIR bioluminescence emission could potentially reach 850 nm. However, in the bioluminescence assay, luciferins **9** and **10** were "dark" with wild type luciferase. Further studies with a complimentary designed luciferase showed light emission for PhOH-Luc **9** at λ_{blu} = 608 nm and additionally gave a broad spectrum in which about 31% of the emission was in the nIR region. In this paper we report the synthesis, photophysical and bioluminescence properties of our own H-bonded rotation restricted π-extended *infra*-luciferin derivative that effectively reduces the degrees of freedom around both of the linking groups single bonds and report its photophysical features.

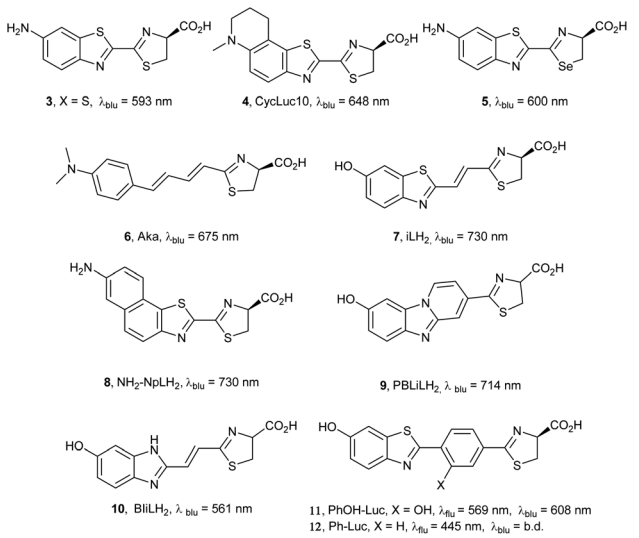

Fig. 1 Representative synthetic D-luciferin analogues with their bioluminescence wavelengths.

Results and discussion

Design and synthesis

By considering the previously discussed modifications of D-Luciferin analogues (stronger intramolecular charge transfer,

extended π-system, rigidification), we set out to design and synthesise a fully rotationally restricted D-luciferin analogue, enamine luciferin **13** (Fig. 2), based on the structure of iLH_2.[21] To the best of our knowledge, there is no example of a fully rotationally restricted D-luciferin analogue. We postulated that full rigidification can be achieved by two intramolecular hydrogen bonds between an enamine -NH_2 group and the two nitrogen atoms in each of the benzothiazole and thiazoline rings. This design maintains the alkene linker between the two heterocycles, the extended π-system, which we have shown has a dramatic effect on the red shifting of bioluminescence emission. The two hydrogen bonds reduce the rotational degrees of freedom around each of the σ-bonds linking the alkene spacer to the heterocyclic rings, rigidifying the system. In addition, **13** possesses an additional electron donating NH_2 substituent in comparison to infraluciferin (**7**) which may provide better intramolecular charge transfer for longer wavelength emission. The introduction of this conformational restraint causes the sulfur atoms of the enamine-infraluciferin analogue **13** to sit in the *cis* position. In contrast, the crystal structures of D-luciferin and iLH_2 transition state mimics in the luciferase enzyme showed that the conformer where the two sulfur atoms adopt a *trans* relationship is the most likely emissive conformation.[22,26–28] We were therefore interested in investigating the bioluminescence emission of the fully rotationally restricted enamine-infraluciferin (**13**). To avoid any unwanted epimerisation of the carboxylic acid, the racemic form of luciferin **13** was synthesised for comparison to D-LH_2 **1** and racemic iLH_2 **7**.

The synthesis began with the protection of the phenol group of known benzothiazole **17**[29] as its triisopropylsilyl ether **18** in quantitative yield (Scheme 2). Treatment of nitrile **18** with anionic acetonitrile solution provided enamine **19** *via* a Thorpe reaction[30,31] in 83% yield. The triisopropylsilyl protecting group was cleaved under mild conditions to give the nitrile precursor **20** in quantitative yield. The final step was biomimetic formation of the thiazoline by treatment with cysteine, but this proved to be a challenging step. Standard reaction[12] of nitrile **20**, racemic cysteine hydrochloride (1.1 eq.), and K_2CO_3 (1.1 eq.) did not provide the desired product. Therefore, solvent and temperature screens were attempted to find suitable conditions (Table S1†). It was found that cyclization could be achieved with anhydrous methanol as solvent and heating the reaction at 80 °C overnight to give luciferin **13** in an isolated yield of 20%.

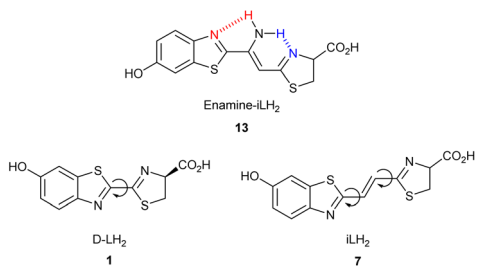

Fig. 2 The structures of racemic luciferin **13**, D-LH_2 **1** and iLH_2 **7**.

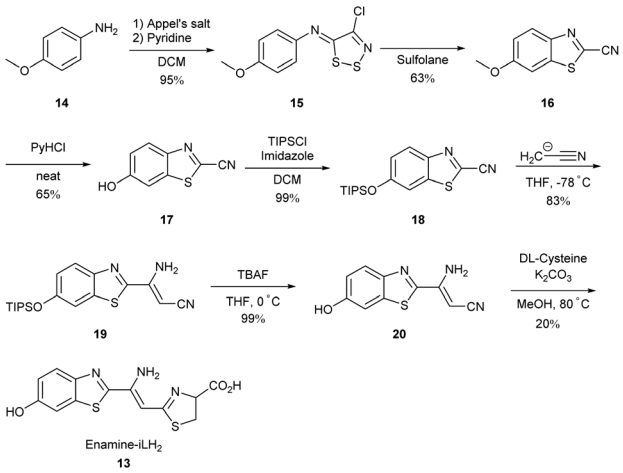

Scheme 2 The synthesis of novel Enamine-iLH_2 13.

Spectroscopic properties

The spectroscopic data of Enamine-iLH_2 (**13**) was collected alongside that of D-luciferin (**1**) and infraluciferin (**7**) for comparison purposes. Absorption spectra were measured in dilute solutions of anhydrous DMSO at 298 K (Fig. 3).

The absorption wavelengths of the luciferins in DMSO were in the order Enamine-iLH_2 **13** (λ_{abs} = 360 nm) > iLH_2 **7** (λ_{abs} = 348 nm) > D-LH_2 **1** (λ_{abs} = 318 nm) (Table 1). The extinction coefficients (ε) of each luciferin were determined as LH_2 **1** (79 200 $M^{-1}cm^{-1}$) > Enamine-iLH_2 **13** (76 000 $M^{-1}cm^{-1}$) > iLH_2 **7** (66 500 $M^{-1}cm^{-1}$). To achieve the most intense emission spectra the maximum absorption wavelength was used to excite these fluorophores. The emission spectra showed the same trend of absorption, Enamine-iLH_2 **13** (λ_{em} = 496 nm) > iLH_2 **7** (λ_{em} = 470 nm) > LH_2 **1** (λ_{em} = 446 nm). The shortest wavelength of LH_2 **1** can be ascribed to the absence of the π-extending alkenyl linker group. Although luciferins iLH_2 **7** and Enamine-iLH_2 **13** bear the same π-extended system, Enamine-iLH_2 **13** gave a longer emission wavelength than iLH_2

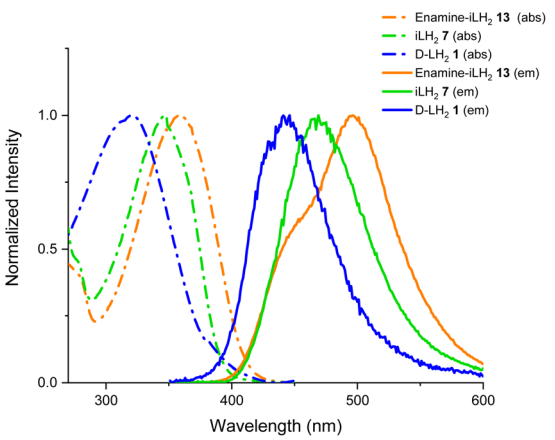

Fig. 3 The normalised absorption and emission spectra of D-luciferin and its analogues in DMSO.

Table 1 Spectroscopic properties of luciferins

Luciferins	λ_{abs} (nm)	ε (M^{-1} cm^{-1})	λ_{em} (nm)	E_{0-0} (eV)
LH_2 **1**	318	79 200	446	3.22
iLH_2 **7**	348	66 500	470	3.08
Enamine-iLH_2 **13**	360	76 000	496	3.01

Absorption and fluorescence emission were recorded in anhydrous DMSO solutions at 298 K. The concentrations for absorption and fluorescence were 10^{-5} M. Band gap E_{0-0} was measured from the intersection of the absorption and emission spectra, $E = 1240/\lambda_{opt}$.

7 by 26 nm with a distinct blue-shift shoulder. Based on the excited state intramolecular proton transfer (ESIPT) mechanism,[32–35] the enamine **13** might contribute to the shoulder emission ranging from 400 to 470 nm, and the longer wavelength emission at 496 nm might be from the tautomer imine **21** form (Fig. 4). Additionally, enamine-iLH_2 **13** has a more planar structure rigidified by the intramolecular H-bonds, improving its conjugation over less rigid **7** in their excited states, which would promote a more red-shifted emission of **13**.[25] The band gaps (E_{0-0}) of each luciferin were estimated from the intersection of the normalised absorption and emission spectra (λ_{opt}).[36–38] The data suggested that Enamine-iLH_2 **13** has the narrowest band gap (3.01 eV) which ascends to iLH_2 **7** (3.08 eV) and LH_2 **1** (3.22 eV). From these spectroscopic characteristics, it was expected that **13** could generate an interesting bioluminescence result.

Computational studies

Computational modelling was applied to investigate whether the intramolecular hydrogen bonds could rigidify luciferin **13**. Four possible conformations were examined using QChem5.4,[39] fully-restricted **13**, partially restricted **13a** and

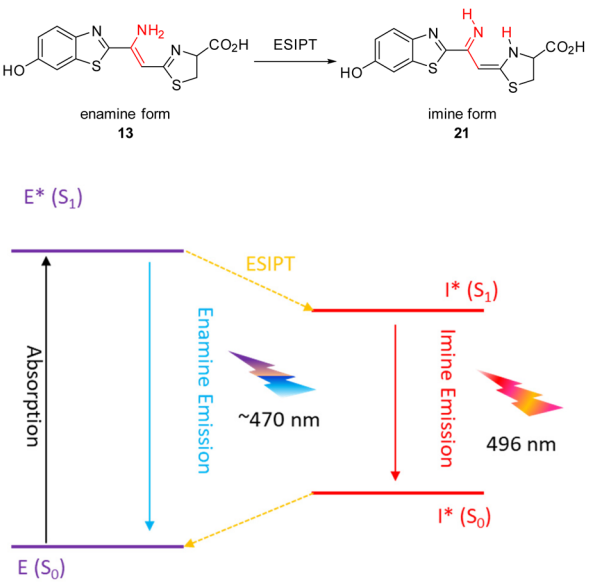

Fig. 4 Plausible enamine imine tautomerization *via* ESIPT process.[32,33]

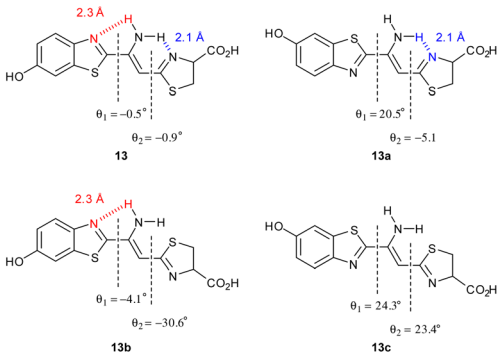

Fig. 5 Calculated hydrogen bond distances and dihedral angles of possible hydrogen bonded conformers.

13b, and flexible **13c** (Fig. 5). The geometry optimizations of each conformation were calculated using DFT with the ωB97X-D3 functional and the def-SVP basis set with PCM method in DMSO to obtain the lowest energy. For the conformers that have H-bond interactions, the distances of the enamine hydrogen bond donor and the benzothiazole acceptor was approximately 2.3 Å. The H-bond interaction between thiazole and the enamine group was 2.1 Å. The computational results also showed that the fully-restricted **13** had the lowest energy along with the smallest torsion angles (θ_1 = −0.5° and θ_2 = −0.9°), due to the two bridged H-bond interactions. In contrast **13c**, which has no intermolecular H-bonding, had the highest energy owing to its highly-twisted conformation disabling conjugation. When compared to coplanar structure **13**, the relative energies calculated by the degree of rigidification *via* hydrogen bond(s) showed that **13a–c** have higher energies at ~15 kJ mol^{-1}, ~44 kJ mol^{-1}, ~49 kJ mol^{-1}, respectively. The computational calculation and the spectroscopic observation (Fig. 3) suggested enamine **13** possesses a planar conformation, restricted by intramolecular H-bonds and is the most stable conformation in the solvent DMSO.

Fully-restricted luciferin **13** had the most red-shifted photoemission among the three luciferins (**1**, **7**, **13**) from our spectroscopic studies. Therefore, we expected that their oxidised forms (**22**, **23**, and **24**) (Fig. 6) would show a corresponding trend with respect to their absorption and emission spectra. Oxy luciferins are notoriously unstable[40] so to test this hypothesis, computer-aided calculations were employed to estimate these compounds' basic electronic transition and spectroscopic properties. The method of choice to describe excitation and emission energies was TDA-TDDFT with the ωB97-X-D3 functional and the def2-SV(P) basis set. For the simulation of the H_2O solvent, the absorption vertical energies were modi-

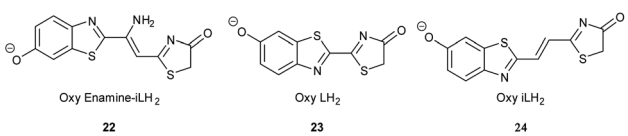

Fig. 6 Deprotonated Oxidized forms of luciferins.

fied with the (ptSS+LR)-PCM method,[41] as this method was able to account for the dynamical response of the fast component of the solvent polarisation (ptSS) and excitonic coupling and dispersion effects (LR). For the excited state optimizations and emission energies the LR-PCM method was used, with the assumption that the solvent molecules have time to reorient in response to changes in the solute's geometry. The ΔE_{abs} (eV) values of oxy luciferins exhibited a slightly different trend to those measured for the parent luciferins; **22** (2.30 eV), **23** (2.84 eV), and **24** (2.39) (Table 2). This demonstrated that **22** had the smallest excitation energy. From ΔE_{em} (eV) and the dipole moment difference $\Delta\mu_{ge}$, **22** has the smallest energy gap and largest change of the $\Delta\mu_{ge}$ (1.80 eV/2.90 Debye), when compared to **23** (2.44 eV/1.25 Debye) and **24** (2.03 eV/1.69 Debye). These results suggested that anion **22** has the best ICT in its excited state and is better able to generate more red-shifted emission.[42]

The frontier orbitals of oxyluciferins **22–24** were visualised through the Avogadro platform (Fig. 7).[43] The HOMOs and LUMOs demonstrated that the electron densities were well delocalized on the backbones, which implies that these oxyluciferins have highly conjugated skeletons. Moreover, these oxyluciferins with their push–pull skeleton showed strong ICT characteristics. The HOMOs are mainly located on the hydroxyl benzothiazole moiety and the LUMOs on the thiazolone segment. The route of ICT is from the election rich phenolate group to the electron deficient carbonyl group. It is worth noting that the -NH_2 group on **22** also acts as a second electron donor and contributes electrons to the electron acceptor *via* ICT.

Table 2 Summarised of calculated results

Compounds	ΔE_{abs} (eV)	ΔE_{em} (eV)	μ_g (Debye)	μ_e (Debye)	$\Delta\mu_{ge}$
Oxy enamine iLH_2 **22**	2.30	1.79	16.99	14.09	2.90
Oxy LH_2 **23**	2.84	2.44	9.84	8.59	1.25
Oxy iLH_2 **24**	2.39	2.03	11.44	9.75	1.69

ΔE_{abs}: vertical absorption energy; ΔE_{em}: vertical emission energy; μ_g (Debye): dipole moment in the ground state; μ_e (Debye): dipole moment in the excited state; $\Delta\mu_{ge}$: Dipole moment change between ground state and excited state.

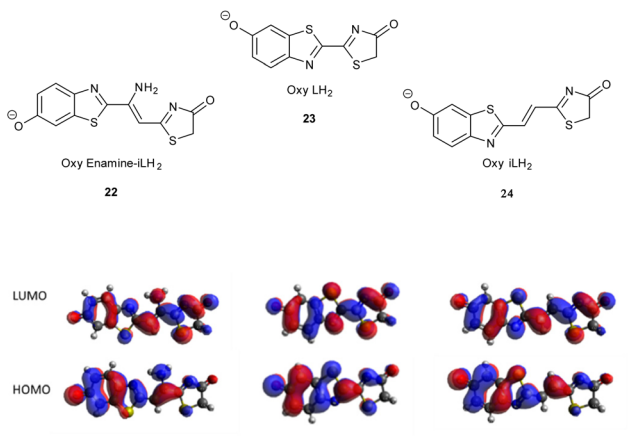

Fig. 7 Selected frontier orbitals of the oxy luciferins **22**, **23**, **24** (isovalue = 0.007 e^3·Bohr^{-1}).

Bioluminescence

The bioluminescence results of luciferins D-LH_2 **1**, iLH_2 **7** and Enamine-iLH_2 **13** were examined with two luciferases *Photinus pyralis* firefly luciferase (PpyWT) and its mutant FlucRed (a mammalian codon optimized *P. pyralis* Luc variant containing 16 mutations)[22] at pH = 7.4 at 25 °C (Table 3). With D-LH_2, enzymes exhibited their expected wavelengths at 561 nm (PpyWT) and 604 nm (FlucRed). The iLH_2 displayed nIR wavelengths at 705 nm (PpyWT) and 707 nm (FlucRed), respectively. The new analogue Enamine-iLH_2 **13** showed surprisingly similar emission wavelengths to D-LH_2 at 564 nm (PpyWT) and 606 nm (FlucRed).

The normalised bioluminescence emission spectra were depicted in Fig. 8. With enzyme PpyWT, **1** and **13** have very similar spectra which nearly overlap. With FlucRed, Enamine-iLH_2 **13** displayed a broad spectrum with 21% of the spectrum located in the nIR region. The distinct shoulder >700 nm is suggestive of a species capable of nIR emission similar to that of iLH2 with FlucRed.

Docking study

The results of the bioluminescence data with PpyWT for the enamine-iLH_2 **13** showed no shift in the wavelength of emission compared to D-LH_2 **1** despite possessing extended conjugation. This result was inconsistent with the fluorescence data and computational studies for enamine-iLH_2 **13**. Due to these conflicting but interesting results, computational molecular docking between PpyLuc luciferase and enamine-iLH_2 **13** was examined to interrogate the subtle intermolecular interactions

Table 3 Bioluminescence emission maxima and relative activities of Luc/substrate pairs

Luciferase/substrate	Specific activity	BL, 25 °C (λ_{max} ± 2 nm)
PpyWT/no added	<0.0008	––
FlucRed/no added	<0.0005	––
PpyWT/LH_2 **1**	100 ± 4	561 (86)
FlucRed/LH_2 **1**	47.11 ± 2.6	601 (90)
PpyWT/iLH_2 **7**	0.07 ± 0.001	705 (102)
FlucRed/iLH_2 **7**	0.14 ± 0.02	707 (90)
PpyWT/enamine-iLH_2 **13**	0.004 ± 0.002	564 (104)
FlucRed/enamine-iLH_2 **13**	0.001 ± 0.003	606 (108)

Specific activities were obtained from assays at pH 7.4 and 23 °C by monitoring and integrating signal intensity for 2 min using purified enzyme (2.5 μg), 50 μM substrate, 1 mM ATP, and 3 mM $MgSO_4$. The background light emission expressed in specific activity terms with PpyLuc (<0.0008) and with FlucRed (<0.0005) without substrates added. Data are expressed as the mean ± standard deviation and are reported relative to the Luc2/LH_2 value, defined as 100 and were corrected for the spectral response of the CCD detector. Data determined from BL emission spectra measured were obtained as described in the ESI.† Bandwidths at full width at half-maximum values are given in parentheses.

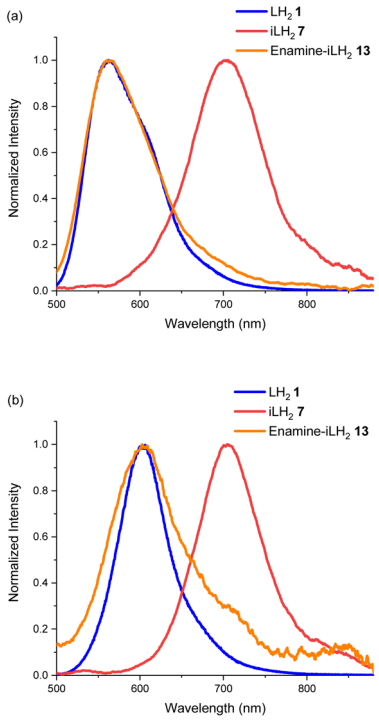

Fig. 8 Normalised bioluminescence emission spectra of luciferins with luciferases (a) PpyWT and (b) mutant luciferase FlucRed.

within the micro-environment of the active site which might affect the bioluminescence wavelength. Such an analysis may also inform the rational design of luciferin/luciferase pairs.

The X-ray cocrystal structures of the active site of PpyLuc luciferase with a luciferin inhibitor LH_2-5′-O-[(*N*-dehydroluciferyl)-sulfamoyl]-adenosine **25** (LH_2-DLSA)[24] and an infraluciferin inhibitor 5′-O-[(N-dehydroinfraluciferyl)-sulfamoyl]-adenosine **26** (iLH_2-DLSA)[22] have previously been determined (Fig. 9). Therefore, adenylated enamine-iLH_2-DLSA **27** is a reasonable ligand candidate to use in molecular docking calculations. Preliminary docking calculations were performed using AutoDock Vina[44] and visualized by Chimera,[45,46] screening the potential binding modes of adenylated **27** with PpyLuc luciferase.

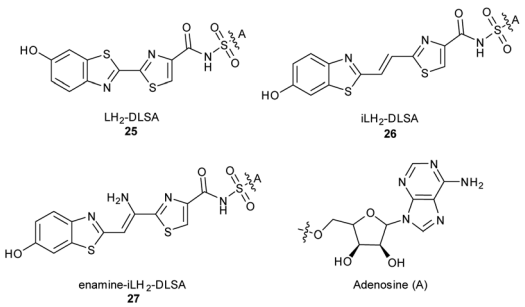

Fig. 9 The structures of LH_2-DLSA **25**, iLH_2-DLSA **26**, and enamine-iLH_2-DLSA **27**.

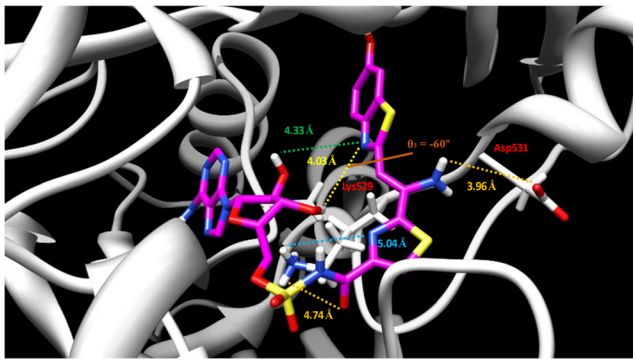

Fig. 10 Preliminary docking study of enamine-iLH_2-DLSA **27** within PpyLuc.

The calculations suggested nine possible conformations readily fit into the PpyLuc active site (Table S2†). The conformation of enamine-iLH_2-DLSA **27** with the lowest affinity energy was chosen to further investigate the H-bond interactions with PpyLuc. From the cocrystals of LH_2-DLSA **25** (Fig. S1†)[26] and iLH_2-DLSA **26** (Fig. S2†)[22] it can be seen that the thiazoline and the benzothiazole rings are planar with respect to each other within the enzyme pocket, allowing π-overlap between them. Unlike LH_2-DLSA **25** and iLH_2-DLSA **26**, the heterocyclic rings of enamine-iLH_2-DLSA **27** appear twisted far from planarity with each other with a torsion angle (θ_3 = −60 °C) (Fig. 10). This unwanted twist can be attributed to the potential interactions among Asp531 with the primary amine (3.96 Å), Lys529 with the nitrogen atom of the thiazoline (5.04 Å), and the intramolecular H-bond interactions between the benzothiazole with the two hydroxyl groups of the adenosine (4.03 Å, 4.33 Å). As a result, the generation of longer emission wavelength was unfavoured due to the poor conjugation. Previous work has shown that Lys529 acts as a hydrogen bond donor to the C=O group of the amide which determines the adenylate reaction and is crucial for its bioactivity.[47] From the cocrystal structures (Fig. S1 and S2†) and our docking prediction (Fig. 10), all the luciferins occupy the active site and bioluminescence is observed, although enamine-iLH_2 exhibited the lowest specific activity (Table 3). The X-ray cocrystal structures of LH_2-DLSA **25** and iLH_2-DLSA **26** showed that the distances between Lys529 to the oxygen atom of the C=O were measured at 1.94 Å, and 2.41 Å, respectively. However, enamine-iLH_2-DLSA **27** had a longer distance (4.74 Å) than the other two luciferins in the docking model. The weaker interaction between enamine-iLH_2-DLSA **27** with Lys529 may account for the lower bioactivity of enamine-iLH_2 **13**.

Conclusions

The first fully conformationally restricted enamine-iLH_2 **13** has been synthesized and subjected to bioluminescence and spectroscopic measurements, and computational and molecular docking calculations. Fluorescence measurements and DFT

calculations support full conformational restriction in the liquid phase and demonstrated that enamine-iLH$_2$ **13** had the smallest band gap and gave the longest fluorescence wavelength in comparison to LH$_2$ **1** and iLH$_2$ **7**. However, the maximum bioluminescence peak of enamine-iLH$_2$ **13** was observed at 564 nm, which is not in line with the emission expected for extended conjugation luciferin substrates. Docking study calculations suggest that the incorporation of the enamine group, although potentially providing planarity and ICT character to the bioluminescent emitter, encourages disadvantageous hydrogen bonding in the micro-environment of the luciferase active site, resulting in the bound structure being significantly non-planar and therefore unable to take advantage of an extended π-conjugation to red shift the emission wavelength. Further study with mutant enzyme FlucRed showed that the bioluminescence emission peak could be shifted to 606 nm with a distinct shoulder above 700 nm. This result implies that enamine-iLH$_2$ can generate nIR photons by mutation of native luciferase. With a suitable mutant luciferase, the enamine luciferin **13** should be able to emit more red-shifted bioluminescence emission than iLH$_2$ **7**.

Experimental

General experimental details - please see ESI†

6-(Triisopropylsilyloxy)benzo[*d*]thiazole-2-carbonitrile (18). To a solution of 2-cyano-6-hydroxybenzothiazole (**17**)[29] (0.20 g, 1.1 mmol), imidazole (0.12 g, 1.8 mmol), and DMF (20 mL) was added TIPSCl (0.32 mL, 1.5 mmol) at rt, and the solution stirred for 24 h. The solution was extracted with EtOAc (3 × 20 mL), the organic layers combined, dried ($MgSO_4$), and filtered. After the volatile materials were removed *in vacuo*, the crude product was purified by column chromatography (silica 80% hexane : 20% EtOAc) to give **18** as a brown oil (0.38 g, 99%). R_f = 0.63 (80% hexane : 20% EtOAc); IR υ_{max} (solution in $CDCl_3$): 2940 (C–H), 2863 (C–H), 2225 (CN), 1594 (C═C), cm^{-1}; ^{1}H NMR (400 MHz, $CDCl_3$) δ 8.04 (1H, d, J = 8.0, ArH), 7.36 (1H, d, J = 4.0, ArH), 7.19 (1H, dd, J = 8.0, 4.0, ArH), 1.31 (3H, sept, J = 8.0, OSiCH(CH_3)$_2$, 1.12 (18H, d, J = 8.0, OSiCH(CH_3)$_2$). ^{13}C NMR (150 MHz, $CDCl_3$) δ 157.4 (ArC), 147.2 (ArC), 137.3 (ArCH), 133.8 (ArCH), 125.9 (ArC), 122.5 (ArC), 113.4 (ArC), 110.8 (ArCH), 18.0 (OSiCH), 12.8 (OSiCH(CH_3)$_2$); HRMS (ESI$^+$) Calcd for $C_{17}H_{25}N_2OSSi$ [M + H]$^+$ 333.1457, found 333.1443.

(*Z*)-3-Amino-3-(6-(triisopropylsilyloxy)benzo[*d*]thiazol-2-yl) acrylonitrile (19). To a solution of acetonitrile (0.070 mL, 1.2 mmol) in an anhydrous THF (1 mL) was added *n*-BuLi (0.76 mL, 1.6 M, 1.2 mmol) at −78 °C and stirred at this temperature for 1 h. This solution was then added dropwise to a solution of **18** (0.25 g, 0.75 mmol) in anhydrous THF (2 mL) at −78 °C under N_2. The mixture was stirred at −78 °C for 1 h and quenched with water. The mixture was extracted with EtOAc (3 × 20 mL), the organic layers were combined, dried ($MgSO_4$), and filtered. After the volatile materials were removed *in vacuo*, the crude product was purified by column chromatography (silica 80% hexane : 20% EtOAc) to give **19** (0.25 g, 83%) as a pale-yellow solid. m.p. 177 °C; R_f = 0.45 (80% hexane : 20% EtOAc); IR υ_{max} (solution in $CDCl_3$): 3458.7 (NH_2), 3321 (NH_2), 2939 (C–H), 2930 (C–H), 2887 (C–H), 2194 (CN), 1618 (C═C) cm^{-1}; ^{1}H NMR (400 MHz, $CDCl_3$) δ 7.87 (1H, d, J = 8.0, ArH), 7.31 (1H, d, J = 4.0, ArH), 7.08 (1H, dd, J = 8.0, 4.0, ArH), 5.63 (2H, s, NH_2), 4.68 (1H, s, C═CH–CN), 1.30 (3H, sept, J = 8.0, OSiCH(CH_3)$_2$, 1.12 (18H, d, J = 8.0, OSiCH(CH_3)$_2$). ^{13}C NMR (150 MHz, $CDCl_3$) δ 158.6 (ArCOSi), 155.8 (CNH_2), 152.6 (ArC), 147.7 (ArC), 136.6 (ArC), 124.7 (ArCH), 121.2 (ArCH), 118.3 (ArCN), 111.4 (ArCH), 66.3 (C═C–CN), 18.0 (OSiCH(CH_3)$_2$), 12.8 (OSiCH(CH_3)$_2$); HRMS (ESI$^+$) Calcd for $C_{19}H_{28}N_3OSSi$ [M + H]$^+$ 374.1722, found 374.1731.

(*Z*)-3-Amino-3-(6-hydroxybenzo[*d*]thiazol-2-yl)acrylonitrile (20). To a solution of **19** (0.20 g, 0.70 mmol), and anhydrous pyridine (20 mL) was added TBAF (2.5 mL, 1.0 M, 2.1 mmol) at 0 °C, and the reaction was stirred for 2 h. After the volatile materials were removed *in vacuo*, the crude product was purified by column chromatography (silica 50% hexane : 50% EtOAc) to give **20** (0.15 g, 95%) as a pale-yellow solid. m.p. 169 °C (dec.); R_f = 0.2 (80% hexane : 20% EtOAc); IR υ_{max} (solution in MeOH): 3448.9 (NH_2), 3369.9 (OH), 2202.7 (CN), 1635.2 (C═C), 1592.9 (N–H) cm^{-1}; ^{1}H NMR (600 MHz, CD_3OD) δ 7.86 (1H, d, J = 8.0, ArH), 7.30 (1H, s, ArH), 7.04 (1H, d, J = 8.0, ArH), 4.70 (1H, s, C═CH–CN). ^{13}C NMR (150 MHz, CD_3OD) δ 159.7 (ArCOH), 158.6 (CNH_2), 155.0 (ArC), 148.0 (ArC), 138.2 (ArC), 125.6 (ArCH) 119.6 (ArCN), 118.0 (ArCH), 107.3 (ArCH), 63.9 (C═C–CN); HRMS (ESI$^+$) Calcd for $C_{10}H_8N_3OS$ [M + H]$^+$ 218.0413, found 218.0388.

Enamine-iLH$_2$ 13. A solution of **20** (10 mg, 50 μmol), D,L-cysteine (6.0 mg, 50 μmol), and anhydrous K_2CO_3 (6.2 mg, 50 μmol) in anhydrous MeOH (1 mL) were stirred at 80 °C for 24 h under N_2. After the volatile materials were removed *in vacuo*, the crude product was purified by reverse phase C18 HPLC with gradient elution (5% Methanol : 95% H_2O followed by 95% Methanol : 5% H_2O) to give Enamine-iLH$_2$ **13** (3.0 mg, 20%) as a pale yellow solid. m.p. 141.6 °C (dec.); IR υ_{max} (solution in $CDCl_3$): 3413 (COOH), 2953 (C–H), 2863 (C–H), 1618 (C═O, C═N, C═C) cm^{-1}; ^{1}H NMR (700 MHz, CD_3OD) δ 7.79 (1H, d, J = 8.0, ArH), 7.25 (1H, s, ArH), 6.98 (1H, d, J = 8.0, ArH), 5.45 (1H, s, NH_2–C═CH), 4.98 (1H, app t, J = 8.0, CH (COOH)), 3.44 (2H, dd, J = 8.0, 4.0, CH_2S). ^{13}C NMR (175 MHz, CD_3OD) δ 179.4 (COOH), 166.8 (C═CH–NCS), 161.9 (NCS), 159.1 (ArCOH), 147.7 (ArC), 146.2 (NH_2–C═CH), 137.8 (ArC), 124.8 (ArCH). 117.9 (ArCH), 107.4 (ArCH), 91.1 (NH_2–C═CH), 83.5 (CHCOOH), 36.5 (CH_2); HRMS (ESI$^+$) Calcd for $C_{13}H_{12}N_3O3S$ [M + H]$^+$ 322.0333, found 322.0320.

Bioluminescence (BL) emission spectra[11]

BL was initiated by mixing equal volumes (0.25 mL) of a solution of 50 mM Tricine pH 7.4 containing 2 mM ATP and 6 mM $MgSO_4$ with a solution of assay buffer containing 12.5 μg of enzyme and 0.1 mM of either LH$_2$ or iLH$_2$ in a quartz cuvette. All solutions were pre-warmed to 25 °C. The final concentrations of the mixture (0.5 mL) in 50 mM Tricine pH 7.4 were 0.4 μM enzyme, 50 μM of the indicated analog, 1 mM ATP, and 3 mM $MgSO_4$. Emission spectra were acquired at 25 °C after a

1 min delay with a Horiba Jobin–Yvon iHR 320 imaging spectrometer equipped with a liquid N_2 cooled CCD detector. Data were collected over the wavelength range 450 nm to 925 nm, with the excitation source turned off and the emission slit width set to 10 nm, and were corrected for the spectral response of the detector using a correction curve provided by the manufacturer. Assay pH values were confirmed before and after spectra were obtained. In order to obtain sufficient signal strength with BL reactions containing Enamine-iLH_2, it was necessary to use 6-fold more enzyme and a slit width of 50 nm.

Specific activities

All assays were performed in triplicate in white 96-well microtiter plates containing 2.5 μg of purified enzyme and 50 μL of 0.1 mM analogue in 50 mM Tricine pH 7.4. BL was initiated by the automated injection of 50 μL of 50 mM Tricine pH 7.4 containing 2 mM ATP, and 6 mM $MgSO_4$. Signals were monitored over 2 min using a Synergy™ 2 microplate luminometer (BioTek, Winooski, VT). Data were integrated and corrected for the spectral response of the Hamamatsu R928 PMT detector.

Author contributions

JCA designed and supervised the project. C-HC performed the chemical synthesis. DF and BRB determined the photophysical and bioluminescence data and interpreted the results. C-HC, SG and PF peformed the computational calculations and docking studies. All authors contributed to writing the paper.

Conflicts of interest

There are no conflicts to declare.

Acknowledgements

We thank the Leverhulme Trust RPG-2019-360 for funding and Dr K. Karu for mass spectra. Mr Aziz Khan (UCL undergraduate project dissertation Chemistry, 2015) is thanked for preliminary studies.

References

1 J. A. Prescher and C. H. Contag, *Curr. Opin. Chem. Biol.*, 2010, **14**, 80–89.
2 C. H. Contag and M. H. Bachmann, *Annu. Rev. Biomed. Eng.*, 2002, **4**, 235–260.
3 S. Y. Teow, K. Liew, M. F. C. Mat, M. Marzuki, N. A. Aziz, T. L. Chu, M. Ahmad and A. S. B. Khoo, *BMC Biotechnol.*, 2019, **19**, 1–11.
4 M. A. Paley and J. A. Prescher, *MedChemComm*, 2014, **5**, 255–267.
5 B. R. Pule, C. E. Behney, T. L. Southworth, D. M. Fontaine, A. M. Gulick, D. J. Vinyard and G. W. Brudvig, *J. Am. Chem. Soc.*, 2015, **137**, 7592–7595.
6 H. H. Seliger and W. D. McElroy, *Proc. Natl. Acad. Sci. U. S. A.*, 1964, **52**, 75–81.
7 Y. Ando, K. Niwa, N. Yamada, T. Enomoto, T. Irie, H. Kubota, Y. Ohmiya and H. Akiyama, *Nat. Photonics*, 2008, **2**, 44–47.
8 B. R. Branchini, T. L. Southworth, N. F. Khattak, E. Michelini and A. Roda, *Anal. Biochem.*, 2005, **345**, 140–148.
9 K. V. Wood, Y. A. Lam, H. H. Seliger and W. D. McElroy, *Science*, 1989, **244**, 700–702.
10 V. R. Viviani, *Cell. Mol. Life Sci.*, 2002, **59**, 1833–1850.
11 B. R. Branchini, D. M. Fontaine, D. Kohrt, B. P. Huta, A. R. Racela, B. R. Fort, T. L. Southworth and A. Roda, *Int. J. Mol. Sci.*, 2022, **23**, 2451.
12 D. C. McCutcheon, M. A. Paley, R. C. Steinhardt and J. A. Prescher, *J. Am. Chem. Soc.*, 2012, **134**, 7604–7607.
13 S. Ioka, T. Saitoh, S. Iwano, K. Suzuki, S. A. Maki, A. Miyawaki, M. Imoto and S. Nishiyama, *Chem. – Eur. J.*, 2016, **22**, 9330–9337.
14 D. K. Sharma, S. T. Adams, K. L. Liebmann, A. Choi and S. C. Moller, *Org. Lett.*, 2019, **21**, 1641–1644.
15 Y. Ikeda, T. Saitoh, K. Niwa, T. Nakajima, N. Kitada, S. A. Maki, M. Sato, D. Citterio, S. Nishiyama and K. Suzuki, *Chem. Commun.*, 2018, **54**, 1774–1777.
16 E. H. White, E. Rapaport, H. H. Seliger and T. A. Hopkins, *Bioorg. Chem.*, 1971, **1**, 92–122.
17 G. R. Reddy, W. C. Thompson and S. C. Miller, *J. Am. Chem. Soc.*, 2010, **132**, 13586–13587.
18 D. M. Mofford, G. R. Reddy and S. C. Miller, *J. Am. Chem. Soc.*, 2014, **136**, 13277–13282.
19 N. R. Conley, A. Dragulescu-Andrasi, J. Rao and W. E. Moerner, *Angew. Chem., Int. Ed.*, 2012, **51**, 3350–3353.
20 S. Iwano, R. Obata, C. Miura, M. Kiyama, K. Hama, M. Nakamura, Y. Amano, S. Kojima, T. Hirano, S. Maki and H. Niwa, *Tetrahedron*, 2013, **69**, 3847–3856.
21 A. P. Jathoul, H. Grounds, J. C. Anderson and M. A. Pule, *Angew. Chem., Int. Ed.*, 2014, **53**, 13059–13063.
22 C. L. Stowe, T. A. Burley, H. Allan, M. Vinci, G. Kramer-Marek, D. M. Ciobota, G. N. Parkinson, T. L. Southworth, G. Agliardi, A. Hotblack, M. F. Lythgoe, B. R. Branchini, T. L. Kalber, J. C. Anderson and M. A. Pule, *eLife*, 2019, **8**, 1–22.
23 M. P. Hall, C. C. Woodroofe, M. G. Wood, I. Que, M. V. Root, Y. Ridwan, C. Shi, T. A. Kirkland, L. P. Encell, K. V. Wood, C. Löwik and L. Mezzanotte, *Nat. Commun.*, 2018, **9**, 132–143.
24 J. C. Anderson, C. H. Chang, A. P. Jathoul and A. J. Syed, *Tetrahedron*, 2019, **75**, 347–356.
25 Z. Yao, B. S. Zhang, R. C. Steinhardt, J. H. Mills and J. A. Prescher, *J. Am. Chem. Soc.*, 2020, **142**, 14080–14089.
26 J. A. Sundlov, D. M. Fontaine, T. L. Southworth, B. R. Branchini and A. M. Gulick, *Biochemistry*, 2012, **51**, 6493–6495.

27 T. Nakatsu, S. Ichiyama, J. Hiratake, A. Saldanha, N. Kobashi, K. Sakata and H. Kato, *Nature*, 2006, **440**, 372–376.
28 D. Dennis and R. H. J. Stanford, *Acta Crystallogr.*, 1973, **B29**, 1053–1058.
29 D. C. McCutcheon, W. B. Porterfield and J. A. Prescher, *Org. Biomol. Chem.*, 2015, **13**, 2117–2121.
30 M. V. Gool, S. A. A. De Diego, O. Delgado, A. A. Trabanco, F. Jourdan, G. J. Macdonald, M. Somers and L. V. Donck, *ChemMedChem*, 2017, **12**, 905–912.
31 H. Baron, F. G. P. Remfry and J. F. Thorpe, *J. Chem. Soc. Trans.*, 1904, **85**, 1726–1761.
32 C.-L. Chen, Y.-T. Chen, A. P. Demchenko and P.-T. Chou, *Nat. Rev. Chem.*, 2018, **2**, 131–143.
33 H.-W. Tseng, J.-Q. Liu, Y.-A. Chen, C.-M. Chao, K.-M. Liu, C.-L. Chen, T.-C. Lin, C.-H. Hung, Y.-L. Chou, T.-C. Lin, T.-L. Wang and P.-T. Chou, *J. Phys. Chem. Lett.*, 2015, **6**, 1477–1486.
34 V. S. Padalkar and S. Seki, *Chem. Soc. Rev.*, 2016, **45**, 169–202.
35 N. Suzuki, K. Suda, D. Yokogawa, H. Kitoh-Nishioka, S. Irle, A. Ando, L. M. G. Abegão, K. Kamada, A. Fukazawa and S. Yamaguchi, *Chem. Sci.*, 2018, **9**, 2666–2673.
36 R. Y.-Y. Lin, F. L. Wu, C. H. Chang, H. H. Chou, T. M. Chuang, T. C. Chu, C. Y. Hsu, P. W. Chen, K. C. Ho, Y. H. Lo and J. T. Lin, *J. Mater. Chem. A*, 2014, **2**, 3092–3101.
37 R. Y.-Y. Lin, H. W. Lin, Y. S. Yen, C. H. Chang, H. H. Chou, P. W. Chen, C. Y. Hsu, Y. C. Chen, J. T. Lin and K. C. Ho, *Energy Environ. Sci.*, 2013, **6**, 2477–2486.
38 C. H. Chang, Y. C. Chen, C. Y. Hsu, H. H. Chou and J. T. Lin, *Org. Lett.*, 2012, **14**, 4726–4729.
39 Y. Shao, Z. Gan, E. Epifanovsky, A. T. B. Gilbert, M. Wormit, J. Kussmann, A. W. Lange, A. Behn, J. Deng, X. Feng, D. Ghosh, M. Goldey, P. R. Horn, L. D. Jacobson, I. Kaliman, R. Z. Khaliullin, T. Kuś, A. Landau, J. Liu, E. I. Proynov, Y. M. Rhee, R. M. Richard, M. A. Rohrdanz, R. P. Steele, E. J. Sundstrom, H. L. Woodcock III, P. M. Zimmerman, D. Zuev, B. Albrecht, E. Alguire, B. Austin, G. J. O. Beran, Y. A. Bernard, E. Berquist, K. Brandhorst, K. B. Bravaya, S. T. Brown, D. Casanova, C.-M. Chang, Y. Chen, S. H. Chien, K. D. Closser, D. L. Crittenden, M. Diedenhofen, R. A. DiStasio Jr., H. Do, A. D. Dutoi, R. G. Edgar, S. Fatehi, L. Fusti-Molnar, A. Ghysels, A. Golubeva-Zadorozhnaya, J. Gomes, M. W. D. Hanson-Heine, P. H. P. Harbach, A. W. Hauser, E. G. Hohenstein, Z. C. Holden, T.-C. Jagau, H. Ji, B. Kaduk, K. Khistyaev, J. Kim, J. Kim, R. A. King, P. Klunzinger, D. Kosenkov, T. Kowalczyk, C. M. Krauter, K. U. Lao, A. D. Laurent, K. V. Lawler, S. V. Levchenko, C. Y. Lin, F. Liu, E. Livshits, R. C. Lochan, A. Luenser, P. Manohar, S. F. Manzer, S.-P. Mao, N. Mardirossian, A. V. Marenich, S. A. Maurer, N. J. Mayhall, E. Neuscamman, C. M. Oana, R. Olivares-Amaya, D. P. O'Neill, J. A. Parkhill, T. M. Perrine, R. Peverati, A. Prociuk, D. R. Rehn, E. Rosta, N. J. Russ, S. M. Sharada, S. Sharma, D. W. Small, A. Sodt, T. Stein, D. Stück, Y.-C. Su, A. J. W. Thom, T. Tsuchimochi, V. Vanovschi, L. Vogt, O. Vydrov, T. Wang, M. A. Watson, J. Wenzel, A. White, C. F. Williams, J. Yang, S. Yeganeh, S. R. Yost, Z.-Q. You, I. Y. Zhang, X. Zhang, Y. Zhao, B. R. Brooks, G. K. L. Chan, D. M. Chipman, C. J. Cramer, W. A. Goddard III, M. S. Gordon, W. J. Hehre, A. Klamt, H. F. Schaefer III, M. W. Schmidt, C. D. Sherrill, D. G. Truhlar, A. Warshel, X. Xu, A. Aspuru-Guzik, R. Baer, A. T. Bell, N. A. Besley, J.-D. Chai, A. Dreuw, B. D. Dunietz, T. R. Furlani, S. R. Gwaltney, C.-P. Hsu, Y. Jung, J. Kong, D. S. Lambrecht, W. Liang, C. Ochsenfeld, V. A. Rassolov, L. V. Slipchenko, J. E. Subotnik, T. V. Voorhis, J. M. Herbert, A. I. Krylov, P. M. W. Gill and M. Head-Gordon, *Mol. Phys.*, 2015, **113**, 184–215.
40 O. V. Maltsev, N. K. Nath, P. Naumov and L. Hintermann, *Angew. Chem., Int. Ed.*, 2014, **53**, 847–850.
41 J. M. Mewes, Z. Q. You, M. Wormit, T. Kriesche, J. M. Herbert and A. Dreuw, *J. Phys. Chem. A*, 2015, **119**, 5446–5464.
42 B. Carsten, J. M. Szarko, H. J. Son, W. Wang, L. Lu, F. He, B. S. Rolczynski, S. J. Lou, L. X. Chen and L. Yu, *J. Am. Chem. Soc.*, 2011, **133**, 20468–20475.
43 M. D. Hanwell, D. E. Curtis, D. C. Lonie, T. Vandermeersch, E. Zurek and G. R. Hutchison, *J. Chem. Inf.*, 2012, **4**, 17.
44 O. Trott and A. J. Olson, *J. Comput. Chem.*, 2010, **31**, 455–461.
45 E. F. Pettersen, T. D. Goddard, C. C. Huang, G. S. Couch, D. M. Greenblatt, E. C. Meng and T. E. Ferrin, *J. Comput. Chem.*, 2004, **25**, 1605–1612.
46 J. E. Chen, C. C. Huang and T. E. Ferrin, *Bioinformatics*, 2015, **31**, 1484–1486.
47 B. B. Branchini, R. A. Magyar, M. H. Murtiashaw and N. C. Portier, *Biochemistry*, 2001, **40**, 2410–2418.